EZH2 Is Essential for Glioblastoma Cancer Stem Cell Maintenance

Mario-Luca Suvà,[1] Nicolò Riggi,[1] Michalina Janiszewska,[1] Ivan Radovanovic,[2] Paolo Provero,[3] Jean-Christophe Stehle,[1] Karine Baumer,[1] Marie-Aude Le Bitoux,[1] Denis Marino,[2] Luisa Cironi,[1] Victor E. Marquez,[4] Virginie Clément,[2] and Ivan Stamenkovic[1]

[1]Division of Experimental Pathology, Institute of Pathology, University of Lausanne, Lausanne, Switzerland; [2]Department of Neurosurgery, University of Geneva, Geneva, Switzerland; [3]Department of Genetics Biology and Biochemistry, University of Turin, Turin, Italy; and [4]Center for Cancer Research, National Cancer Institute-Frederick, Frederick, Maryland

Abstract

Overexpression of the polycomb group protein enhancer of zeste homologue 2 (EZH2) occurs in diverse malignancies, including prostate cancer, breast cancer, and glioblastoma multiforme (GBM). Based on its ability to modulate transcription of key genes implicated in cell cycle control, DNA repair, and cell differentiation, EZH2 is believed to play a crucial role in tissue-specific stem cell maintenance and tumor development. Here, we show that targeted pharmacologic disruption of EZH2 by the *S*-adenosylhomocysteine hydrolase inhibitor 3-deazaneplanocin A (DZNep), or its specific downregulation by short hairpin RNA (shRNA), strongly impairs GBM cancer stem cell (CSC) self-renewal *in vitro* and tumor-initiating capacity *in vivo*. Using genome-wide expression analysis of DZNep-treated GBM CSCs, we found the expression of *c-myc*, recently reported to be essential for GBM CSCs, to be strongly repressed upon EZH2 depletion. Specific shRNA-mediated downregulation of EZH2 in combination with chromatin immunoprecipitation experiments revealed that *c-myc* is a direct target of EZH2 in GBM CSCs. Taken together, our observations provide evidence that direct transcriptional regulation of *c-myc* by EZH2 may constitute a novel mechanism underlying GBM CSC maintenance and suggest that EZH2 may be a valuable new therapeutic target for GBM management. [Cancer Res 2009;69(24):9211–8]

Introduction

Glioblastoma multiforme (GBM), also known as grade 4 astrocytoma, is the most aggressive form of malignant glioma. A diffusely infiltrating tumor, GBM is believed to arise from transformation of neural stem cells (1), and despite aggressive multimodal therapy, remains for the most part incurable, the estimated median survival of affected patients being less than 1 year (2). Identification of new therapeutic targets and strategies to improve the efficacy of existing forms of therapy are therefore urgently needed.

Cancer stem cells (CSC) in human GBM have recently been identified and shown to constitute a primitive cell population capable of self-renewal and differentiation that has the unique capacity to give rise to new tumors upon serial transplantation (3–5). In a subset of GBM, these cells can be enriched by sorting for expression of the surface marker CD133, but their defining properties include *in vitro* spherogenic potential and *in vivo* tumor-initiating capacity (6). Cancer stem/initiating cells are believed to play an essential role in tumor recurrence after therapeutic intervention (7), and their high chemoresistance and radiation resistance (8) require the identification of alternative therapeutic strategies that could effectively lead to their functional or physical eradication. Although a few signaling pathways, including Sonic-Hedgehog (9), and the bone morphogenic proteins BMP4 and BMPR1B (10, 11) have been shown to be implicated in GBM CSC maintenance, the mechanisms underlying GBM CSC generation, propagation, and chemoresistance have yet to be elucidated. Increasing evidence suggests that polycomb group proteins (PcG) are implicated in regulating CSC pluripotency and survival (12), but their role in GBM CSC has not yet been addressed.

Polycomb group proteins were originally identified in the fruitfly as repressors of *HOX* genes based on mutant phenotypes involving posterior body segment development (12). Functionally, PcG proteins are grouped according to their association with distinct multimeric complexes known as polycomb repressive complexes (PRC). One such group, called PRC2, consists of the association of EZH2 (enhancer of zeste homologue 2), SUZ12 (suppressor of zeste 12), and EED (embryonic ectoderm development), and is involved in the initiation of epigenetic-mediated gene silencing.

EZH2 is the catalytically active component of the PRC2 complex that participates in transcriptional repression of specific genes by trimethylation of lysine 27 and, to a lesser extent, lysine 9 of histone H3 (13). EZH2 is upregulated in a broad range of hematopoietic and solid human malignancies, where its overexpression is associated with poor prognosis (14, 15). A significant number of recently identified PcG target genes are silenced in human tumors by DNA methylation of their promoter. The PRC2 complex could therefore promote tumorigenesis by specifically repressing tumor-suppressor genes, including the major tumor suppressor locus *CDKN2A* (16), through recruitment of DNA methyltransferases. Other studies suggest that an EZH2-associated methyltransferase complex present in the cytoplasm may be implicated in actin polymerization and may influence cellular adhesion and migration, thereby contributing to tumor dissemination. PcG proteins also play a key role during embryogenesis, as evidenced by the observations that targeted disruption of the PRC2 member *EZH2* results in early embryonic lethality (17) and that *EZH2*-deficient embryonic stem cell lines cannot be established *in vitro* (18). Interestingly, the promoters of a significant proportion of PcG target genes in embryonic stem cells are also co-occupied by Oct-4, Sox-2, and Nanog, three transcription factors that are essential in sustaining stem cell pluripotency.

Based on its role in stem cell maintenance and tumor growth promotion, we assessed the effect of targeting EZH2 in human GBM CSCs. Recent work has shown that 3-deazaneplanocin A

Note: Supplementary data for this article are available at Cancer Research Online (http://cancerres.aacrjournals.org/).

M.-L. Suvà and N. Riggi contributed equally to this work.

Requests for reprints: Ivan Stamenkovic, University of Lausanne, 25 Rue du Bugnon, Lausanne CH-1011, Switzerland. Phone: 41-21-314-7136; Fax: 41-21-314-7110; E-mail: Ivan.Stamenkovic@chuv.ch.

doi:10.1158/0008-5472.CAN-09-1622

(DZNep), one of the most potent *S*-adenosylhomocysteine inhibitors, depletes cellular levels of the PRC2 components EZH2, SUZ12, and EED and blocks the associated histone H3 lysine 27 methylation (19). One apparent consequence of these effects is the induction of apoptosis in malignant but not in normal cells (19). Here, we show that DZNep-based pharmacologic disruption of EZH2 as well as short hairpin RNA (shRNA)–mediated downregulation of EZH2 expression in GBM CSC dramatically reduces their clonogenic potential *in vitro* and tumor-initiating ability *in vivo*, providing evidence that PRC2 complexes may represent an effective and hitherto unrecognized therapeutic target in the clinical management of GBM.

Materials and Methods

Tumor samples, CSC culture, viability, bromodeoxyuridine, and clonogenic assay. Tumor samples of GBM from three patients undergoing surgical biopsies (Supplementary data 1*A*) were obtained directly after surgical removal in accordance with local legislation (HUG protocol 04-113). Single-cell suspensions, freshly isolated from tumor samples, were cultivated in DMEM-F12 (Gibco), supplemented with 20% BIT (Stem Cell Technologies) or B27 (1/50 Invitrogen), 10 ng/mL recombinant human epidermal growth factor (EGF; Invitrogen), 10 ng/mL recombinant human basic fibroblast growth factor (FGF; Invitrogen), and 1% penicillin/streptomycin (Gibco). As previously described (3, 4, 6, 20), nonadherent cellular spheroids derived from these serum-free culture conditions were considered as enriched CSC cultures and were used for subsequent experiments. When DZNep (21) or temozolomide was added to the culture, CSC spheres were grown in growth factor–reduced medium, containing 1 ng/mL EGF and 1 ng/mL FGF. Viability of the cells was assessed by adding trypan blue (1/3,000) to freshly disaggregated GBM CSC spheres and rapidly analyzing samples by FACS using FL3 laser in a FACSCalibur apparatus (Becton Dickinson). Bromodeoxyuridine (BrdUrd) incorporation was assessed according to the manufacturer's instructions. For clonogenic assays, disaggregated GBM CSC spheres were plated as single cells in 10 × 96-well plates and cultivated for 2 wk in serum-free medium devoid of any drug (DZNep or temozolomide). Fresh medium was added every 5 d to renew the growth factor supply.

Human GBM cell lines and adherent primary cultures. Glioblastoma cell lines LN18, T98, and U87MG (kindly provided by Dr. Monika Hegi) were grown in DMEM (Gibco) supplemented with 10% fetal bovine serum (FBS; Gibco) and 1% penicillin/streptomycin (Gibco). Adherent primary cultures (differentiated BT-2 and BT-3) were obtained by growing tumor cells freshly isolated from GBM samples in DMEM-F12 (Gibco), supplemented with 10% FBS (Gibco) and 1% penicillin/streptomycin (Gibco).

EZH2 knockdown and retroviral infection. The sequences of the two different 21-nucleotide shRNAs targeting the human EZH2 sequence were previously described (22). Sense and antisense oligonucleotides were annealed to form duplexes and inserted into the pSIREN-Retro Q retroviral vector (BD Biosciences Clontech), according to the manufacturer's recommendations, published in the retroviral gene transfer and user manual. Briefly, plasmids containing EZH2 or control shRNA were transfected into GP2 packaging cells to produce the virus used to infect the target gliomaspheres. Viral supernatant was concentrated by ultracentrifugation, using a SW28 rotor (Beckman Coulter), at 19,500 rpm for 90 min. Two rounds of infection, at 24-h intervals, were performed by adding concentrated virus to dissociated spheres. Forty-eight hours after the second round, cells were selected for puromycin (2 μg/mL) resistance for 5 d. The degree of EZH2 knockdown was then assessed by real-time quantitative PCR and Western blot analysis.

Nonobese diabetic–severe combined immunodeficient mice xenotransplantation and survival analysis. For intracranial xenografts, gliomaspheres (500 cells) were implanted at coordinates $x = -2$, $y = 0$, $z = -2$ relative to the bregma point with a sterotaxic apparatus (Kopf Instruments). *P* values for differences in survival were obtained with a log-rank test. Experimental procedures involving mice were approved by the Etat de Genève, Service Vétérinaire, authorization number 1007/3337/2.

Affymetrix GeneChip array analysis and statistical analysis of the expression data. After 5 d of DZNep treatment, total RNA was extracted from each of the three treated primary cultures and their respective controls, using the RNeasy Mini Kit (Qiagen) according to the manufacturer's recommendations. The quality of total RNA was verified by an Agilent RNA 600 nanoassay and by measuring the 260/280 absorbance ratio. The corresponding quality-tested total RNA was used by the Lausanne DNA Array Facility to perform gene expression profile analysis using the Affymetrix HG-U133 Plus 2.0 Arrays, following the manufacturer's recommendation (for further details, go to the Web site[5]). For each of the three freshly isolated batches of BT-CSC, Affymetrix analysis was performed by comparing BT-CSC treated with DZNep with their respective control. Normalization and background subtraction were performed with RMA (Irizarry2003) using the "affy" package of Bioconductor (Gentleman2004). Probe sets showing a fold change >2 or <1/2 in all the three samples were retained for further analysis. The gene expression data are accessible from the Gene Expression Omnibus[6] under accession GSE18150.

Gene Ontology enrichment analysis. The lists of induced and repressed probe sets were translated into Entrez gene IDs using the annotation files provided by Affymetrix (version na26). Only probe sets associated to a single Entrez gene ID were considered. Gene Ontology (GO) annotations of human genes were obtained from the Entrez gene database (downloaded on December 9, 2008). Overrepresentation of GO annotations was evaluated with an exact one-sided Fisher's test, with Bonferroni correction for multiple testing.

Western blot. Cell lysis, SDS-PAGE, membrane blotting, and immunostaining were performed by standard procedures and protein bands were detected using a chemiluminescent substrate kit (Pierce) according to the manufacturer's recommendations. Primary rabbit anti-EZH2 polyclonal (Cell Signaling) and mouse anti-MYC monoclonal (Invitrogen) antibodies were used. Secondary antibodies were horseradish peroxidase (HRP)–conjugated goat anti-mouse (Bio-Rad) and mouse anti-rabbit (Sigma) antibodies. Western blot band intensity quantification was performed using IMAGE J Software.

Immunohistochemistry. Paraffin-embedded sections of glioblastomas were stained with rabbit anti-human EZH2 (1:50 Dilution, Cell Signaling). HRP staining was performed using biotin-conjugated goat anti-rabbit IgG (Vector Laboratories) and revealed with a DAKO DAB Kit (DAKO).

Chromatin immunoprecipitation. Starting with 20×10^6 cells cultured as spheres, chromatin immunoprecipitation (ChiP) was performed following standard procedures using 1% paraformaldehyde as a cross-linking agent. Five micrograms of anti-Suz12 antibody (ab12073, Abcam) or of the isotype-control antibody (rabbit IgG, Dako) were used for the assay. To analyze the precipitated DNA, real-time quantitative PCR was performed using specific primers (see below).

Real-time quantitative reverse transcriptase-PCR. For gene expression assays, cDNA was obtained using Moloney murine leukemia virus reverse transcriptase and RNase H minus (Promega). Typically, 250 ng of template total RNA and 250 ng of random hexamers were used per reaction. Real-time PCR amplification was performed using a Taq Man Universal PCR mastermix and Assays-On-Demand gene expression products or Power SYBR mix and specific PCR primers, in an ABI Prism 7900 instrument (Applied Biosystems). Relative quantification of each target, normalized to an endogenous control (cyclophylin A), was performed using a comparative Ct method (Applied Biosystems). Probes used included human MYC, EZH2, and BMPR1B (Assays-On-Demand gene expression, Applied Biosystems). For ChIP experiments, the following specific primers were used: for human MYC promoter amplification: TCCTCTCTCG CTAATCTCCGC and CCCTCCGTTCTTTTTCCCG, normalized to human neutrophil elastase promoter: TGAATGCGATTGTGCATCCTG and AGGACACAGGCGAGGAAAAGAC.

[5] http://www.unil.ch/dafl/
[6] http://www.ncbi.nlm.nih.gov/geo/

Results and Discussion

EZH2 is strongly expressed in glioblastoma samples and its pharmacologic inhibition impairs GBM CSC self-renewal *in vitro* and delays tumor initiation *in vivo*. Assessment of EZH2 expression by immunohistochemistry in paraffin-embedded samples of GBM revealed elevated expression in tumor cells (five of five samples) but no detectable expression in adjacent brain parenchyma (Fig. 1*A, left* and data not shown). These observations are consistent with previous reports (23) and with the notion that EZH2 is amplified in a wide range of human malignancies. To study its role in GBM CSC biology, we derived primary CSC cultures from three unrelated human GBM samples (Supplementary data 1*A*) by allowing expansion, in serum-free conditions, of freshly isolated single-cell suspensions into cellular spheroids, as previously described (20). Primary cultures of GBM CSCs (henceforth BT-CSC) were then subjected to *in vitro* treatment with the PRC2 inhibitor compound DZNep at 5 μmol/L, a concentration that has been shown to be sufficient to disrupt PRC2 complexes and to trigger apoptosis in cancer cell lines within 48 to 72 hours, while being harmless to untransformed cells (19). As reported, treatment with 5 μmol/L DZNep resulted in the reduction of EZH2 protein expression levels (Fig. 1*A, middle*). DZNep treatment also altered sphere morphology (Fig. 1*A, right*), but had no significant effect on BT-CSC viability, even after 5 days of *in vitro* treatment (Fig. 1*B, left*). Based on the well-established role of EZH2 in cell cycle progression, we assessed the effect of the drug on *in vitro* cell proliferation. BT-CSC treated with DZNep showed only a moderate reduction of their proliferation rate, as illustrated by a limited 20% decrease in their BrdUrd incorporation (Fig. 1*B, right*). To evaluate the effect of DZNep treatment on BT-CSC self-renewal, we performed a clonogenic assay. Gliomaspheres were treated with 5 μmol/L DZNep for 5 days, then disrupted and plated as

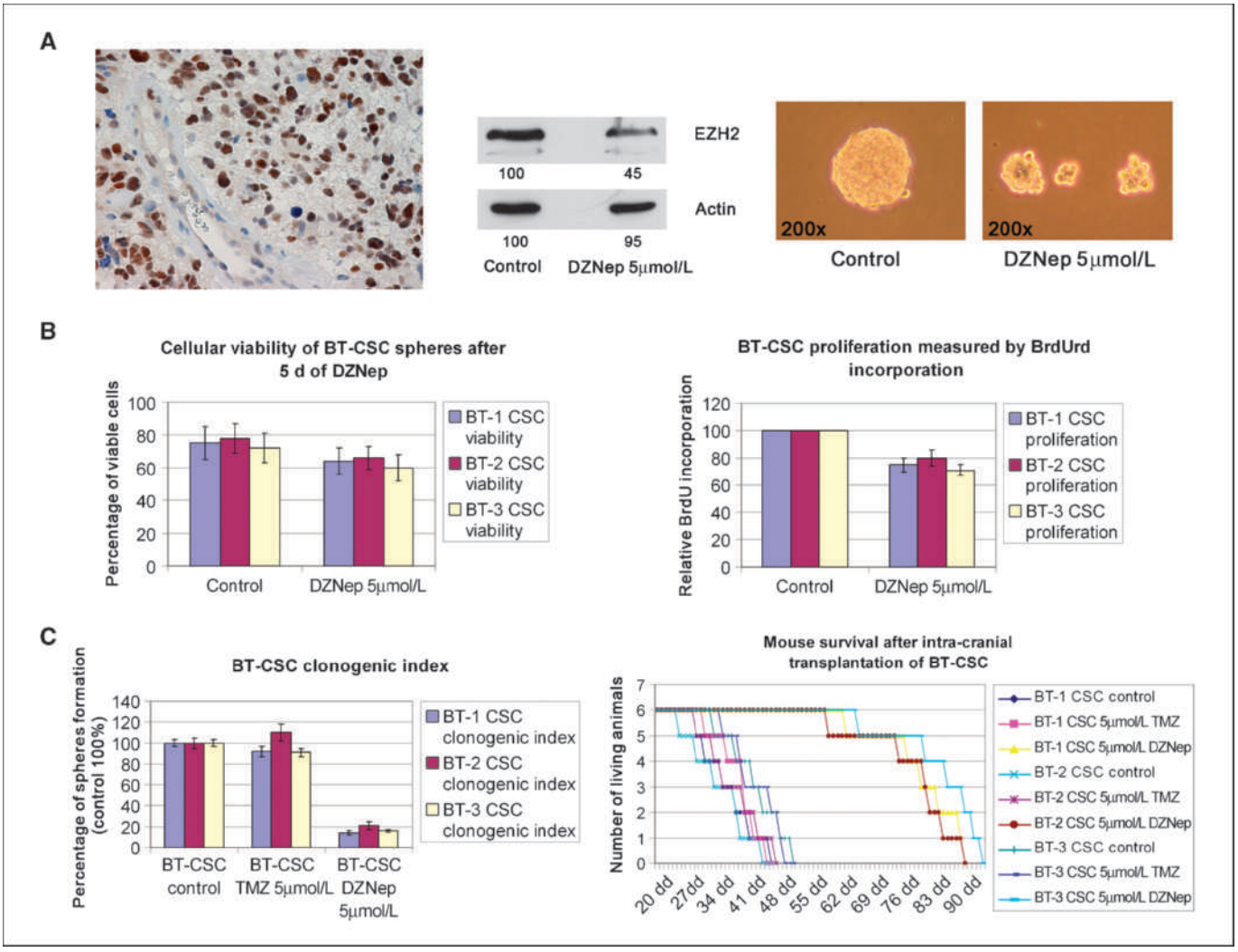

Figure 1. Pharmacologic depletion of EZH2 reduces the self-renewal and tumor-initiating properties of GBM CSCs. EZH2 expression in primary human glioblastoma samples (*A, left*). Treatment of GBM CSC spheres with 5 μmol/L of DZNep for 5 d reduces EZH2 protein levels, as assessed by Western blot analysis (*A, middle; numbers,* relative band intensity) and alters sphere shape (*A, right*). DZNep at 5 μmol/L for 5 d does not significantly impair GBM CSC viability (*B, left*) or proliferation (*B, right*). GBM CSC treated with 5 μmol/L DZNep or temozolomide (*TMZ*) were assessed for their CSC properties, namely clonogenic index (*C, left*) and tumor-initiating potential (*C, right*), compared with their solvent-treated counterparts, demonstrating that DZNep but not temozolomide treatment efficiently decreases the clonogenic index of GBM CSC and extends the survival of all the animals injected with the corresponding cells. Mouse survival *P* values from log-rank test: DZNep versus control: BT-1 (0.000506), BT-2 (0.000506), and BT-3 (0.000506); temozolomide versus control: BT-1 (0.828), BT-2 (0.417), and BT-3 (0.817). DZNep versus temozolomide: BT-1 (0.000526), BT-2 (0.000506), and BT-3 (0.000506). *Error bars,* SD of three independent determinations.

single-cell suspensions in CSC medium without DZNep, to assess their sphere-forming ability (see Materials and Methods for details). Interestingly, the clonogenic index was diminished by >80% in all samples whereas the same assay performed in the presence of 5 μmol/L temozolomide, the principal cytotoxic drug currently used for GBM, revealed virtually no reduction of BT-CSC clonogenicity (Fig. 1*C, left*). This observation is consistent with recent work showing that impairment of glioma CSC self-renewal requires at least 50 μmol/L of temozolomide, a concentration that is 10 times higher than the therapeutic dose used in the clinic (24).

To determine the effect of a short 5-day *in vitro* treatment of BT-CSC with DZNep or temozolomide on their tumor-initiating potential, we performed intracranial injection of BT-CSC into immunocompromised mice. Injection of 500 control (solvent) and temozolomide-treated BT-CSC resulted in death of the animals within 25 to 50 days, with no benefit (nonsignificant *P* values) from temozolomide (Fig. 1*C, right*). By contrast, treatment of BT-CSC with 5 μmol/L DZNep before injection significantly extended the survival of all the animals (Fig. 1*C, right*; *P* values of 0.0005 for each BT-CSC population), suggesting that the short *in vitro* DZNep treatment was sufficient to decrease the number of tumor-initiating cells in all the BT-CSC samples, resulting in delayed tumor development.

Abrogation of EZH2 function induces transcriptome changes consistent with the implication of EZH2 in epigenetic regulation of gene expression. Our observations suggest that DZNep treatment selectively abrogated clonogenicity of GBM CSC and impaired their tumor-initiating potential. To identify EZH2-regulated genes that may be required for clonogenicity and tumorigenesis of these cells, we analyzed global gene expression profile changes in BT-CSC following 5 days of DZNep treatment. Because the phenotype of the three primary cultures tested was highly similar, we considered only those transcripts whose movement was consistently shared among all three samples. Thus, 823 common genes were observed to be induced (fold change >2) and 508 to be repressed in all three samples (Supplementary data 2). The top 25 induced and repressed genes, ranked according to average fold change, are shown in a heatmap in Fig. 2*A*. Interestingly, *c-myc* was among the top transcripts that were downregulated by DZNep treatment (Fig. 2*A, arrow*). Overrepresented GO terms among repressed genes included mitochondrion, mitochondrial part, transport, and transporter activity (Fig. 2*B, top*). Overrepresented GO terms among upregulated genes included chromosome, chromosome part, terms related to chromatin and chromatin structure, nucleosome organization, chromatin assembly, and protein-DNA complex, consistent with known epigenetic functions of EZH2 (Fig. 2*B, bottom*).

***C-MYC* is a target gene of EZH2 in GBM CSCs and can partially rescue their DZNep-induced loss of clonogenic potential.** Microarray analysis revealed downregulation of *c-myc* in all three DZNep-treated BT-CSC populations tested. Recent work has shown that *c-myc* is highly expressed in glioma CSC (25, 26) and that its targeted depletion reduces CSC proliferation and increases their susceptibility to proapoptotic signals, suggesting that *c-myc* may play a key role in glioma CSC maintenance and survival. These observations are consistent with the notion that *c-myc* is one of the central genes implicated in genetic reprogramming (27). Downregulation of *c-myc* in BT-CSC by the pharmacologic agent DZNep therefore seems to be an important event that may explain, at least in part, the observed decrease in clonogenic and tumorigenic potential; among the top DZNep-deregulated genes, *c-myc* thus seemed to be an appropriate choice for further investigation. Real-time PCR analysis confirmed ~90% depletion of *c-myc* transcripts in DZNep-treated BT-CSC that correlated with a robust depletion of the protein (Fig. 3*A, left* and *middle*). Importantly, temozolomide had no effect on either *c-myc* transcript or protein expression (Fig. 3*A, left* and *middle*). To determine whether the effect of DZNep on *c-myc* is specific to CSC, we examined the effect of DZNep on glioblastoma cells grown as adherent monolayers in serum-supplemented medium, which constitute well-established conditions to convert CSC spheres into more differentiated cells with limited tumor-initiating capacity. To that end, we cultivated three GBM cell lines and two primary GBM cultures in serum-supplemented medium and treated them for 5 days with 5 μmol/L DZNep. Remarkably, DZNep had no effect on *c-myc* expression in any of these five cell cultures (Fig. 3*A, right*), suggesting a GBM CSC–specific effect of DZNep; this is consistent with published results on the treatment of established cancer cell lines with DZNep where no effect on *c-myc* has been reported (19).

We next asked whether *c-myc* might alone be responsible for the observed decrease in clonogenic potential of DZNep-treated BT-CSC. We reasoned that using an exogenous promoter might render *c-myc* expression independent of EZH2. To that end, BT-CSC were infected with a retrovirus expressing *c-myc*, resulting in a moderate (3- to 5-fold) induction of the *c-myc* transcript (Supplementary data 1*B*), probably because of an already high baseline expression level. *c-myc*–infected BT-CSC were subsequently treated for 5 days with 5 μmol/L DZNep. As expected, *c-myc* transcripts and protein expressed from an extraneous retroviral promoter were unaffected by DZNep, as assessed by real-time PCR and Western blot analyses (Fig. 3*B, left* and *middle*). Clonogenic assays revealed that *c-myc*–infected BT-CSC treated with DZNep displayed an ~40% reduction in clonogenic potential compared with untreated cells, whereas empty vector–infected cells displayed >80% reduction (Fig. 3*B, right*), as initially observed in native BT-CSC. These results indicate that *c-myc* can partially rescue DZNep-mediated impairment of BT-CSC clonogenic potential and support its role in CSC self-renewal. The partial rescue, however, indicates that other genes affected by DZNep in BT-CSC are likely to participate in the observed loss of the clonogenic index.

To ensure that the observed depletion of *c-myc* was due to EZH2 disruption and not to some unrelated effect of DZNep, we depleted EZH2 in BT-CSC using two different EZH2-specific shRNAs and assessed the effect on *c-myc* transcripts and c-myc protein. EZH2 downregulation resulted in roughly 80% depletion of *c-myc* transcripts and a robust reduction of c-myc protein (Fig. 4*A, left* and *middle*), further confirming the existence of a functional relationship between EZH2 and *c-myc* levels in BT-CSC.

To determine whether the PRC2 complex binds to the *c-myc* promoter, we performed ChIP experiments using anti-Suz12 antibody, Suz12 being the DNA binding component of the PRC2 complex. Quantitative real-time PCR revealed a 5- to 6-fold enrichment of the *c-myc* promoter in the anti-Suz12 antibody immunoprecipitate compared with that of the isotype control (Fig. 4*A, right*) in BT-CSC. By contrast, the same experiment performed in GBM cell lines showed no enrichment of the *c-myc* promoter in the anti-Suz12 antibody immunoprecipitate (Fig. 4*A, right*). These results imply that the PRC-2 complex directly binds to the *c-myc* promoter in BT-CSC spheres, whereas it fails to do so in GBM cell lines grown in serum-supplemented medium, and are consistent with the absence of an effect of DZNep on *c-myc* transcripts in established cell lines and serum-supplemented medium–grown BT-CSC.

Because the PRC2 complex is mostly a transcriptional repressor, the activating/derepressing effect of Suz12 associated with its

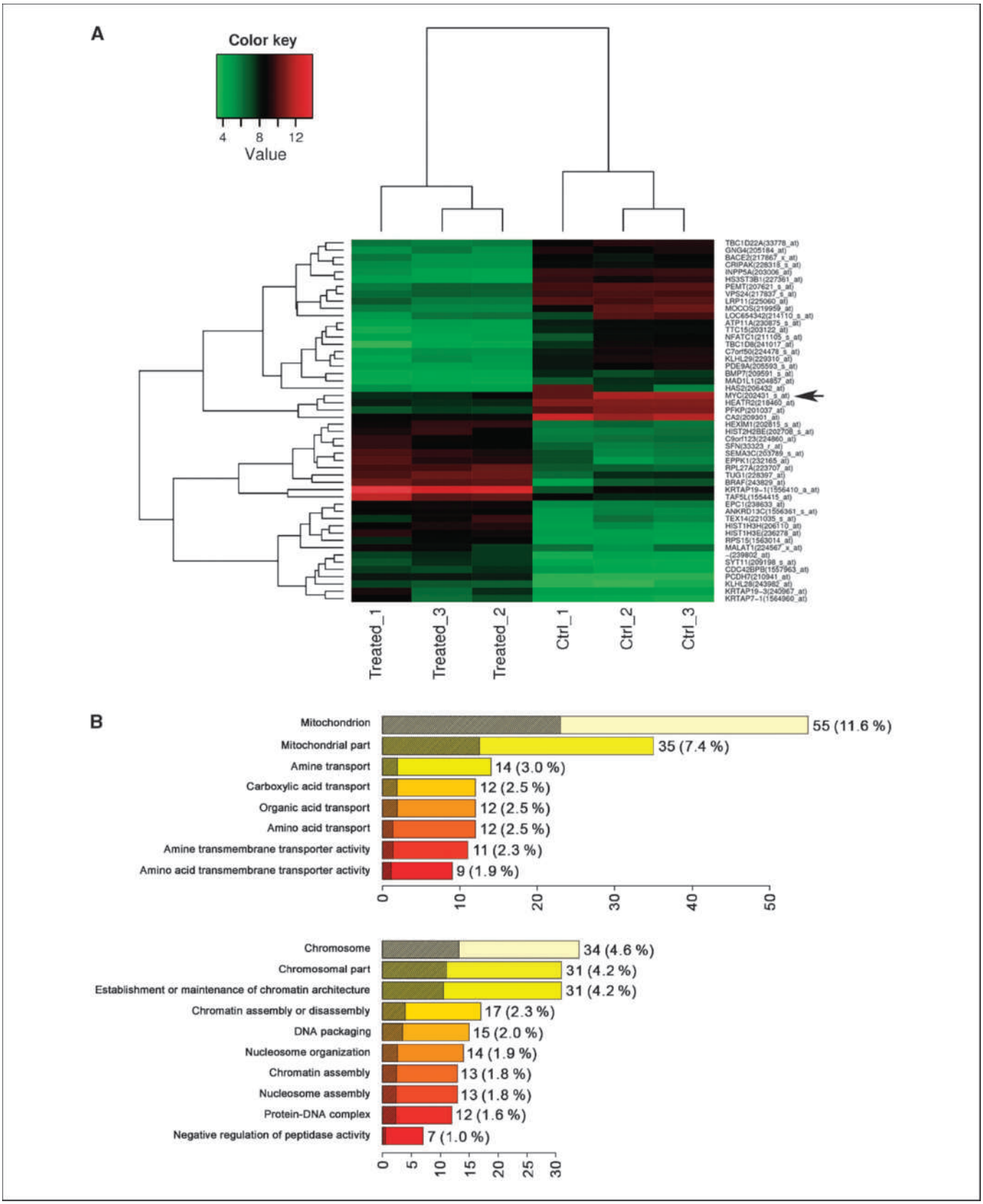

Figure 2. Abrogation of EZH2 function induces transcriptome changes consistent with the implication of EZH2 in epigenetic regulation of gene expression. *A,* heatmap representation of the top 25 induced and repressed genes following 5 d of DZNep treatment, in three different GBM CSC populations (*arrow,* repression of the c-myc transcript). *B,* overrepresented GO terms among repressed (*top*) and induced (*bottom*) genes, showing a significant overrepresentation of GO terms linked to DNA epigenetic modifications among the induced transcripts.

binding to a promoter was unexpected. However, the control of *c-myc* expression is highly complex, and recent data in *Drosophila* point to a hitherto unrecognized mechanism whereby the PcG-related protein Su(z)2 antagonizes *dmyc* autorepression, leading to increased *dmyc* levels (28). Such a scenario could explain the observed drop in *c-myc* levels upon PRC2 disruption in GBM CSCs. It could also be part of a mechanism underlying the high expression level of *c-myc* in GBM CSCs. Whether a direct or indirect consequence, the high number of downregulated genes upon PRC2 depletion in BT-CSC supports the notion that functionally relevant genes, such as *c-myc* in the present model, are positively regulated by PRC2 in GBM CSCs.

GBM CSCs depleted of EZH2 lose tumor-forming capacity. To further assess the effectiveness of EZH2 depletion on the ability of BT-CSC to form tumors *in vivo*, 500 cells of each (BT1-3) BT-CSC population, infected with viruses expressing either EZH2-specific shRNA (two different sequences, targeting different regions of the transcript) or control shRNA, were injected intracranially into immunocompromised mice and the animals were monitored for neurologic signs and survival. Whereas all animals injected with cells containing control shRNAs (6 per BT-CSC population, hence 18 total) died within 45 to 50 days after injection, 32 of 36 animals injected with cells containing EZH2-specific shRNA (6 animals per BT-CSC population and per shRNA, hence 36 total) were alive and symptom-free 100 days following injection when the experiment was terminated (for significant *P* values for each population of BT-CSC and each shRNA, see figure legends; Fig. 4*B, left*). In a parallel experiment, mice were sacrificed at day 35 and the brains were examined for the presence of tumor. Whereas massive tumor growth was observed in all control animals (Fig. 4*B, middle*), no histologically detectable tumor growth was observed in animals injected with cells containing EZH2-specific shRNA (Fig. 4*B, right*).

An almost complete loss of tumor-initiating potential has been recently observed following disruption of *c-myc* in GBM CSCs (25, 26) and the observed *c-myc* downregulation therefore provides a plausible mechanism to explain the loss of tumorigenicity displayed by EZH2-depleted glioblastoma CSCs. However, the mechanistic quantification of the role played by *c-myc*, which could be evaluated by reexpressing *c-myc* with a retroviral system in EZH2-depleted glioblastoma CSC, has proven difficult to achieve due to the susceptibility of BT-CSC to multiple retroviral infections. Recently, EZH2-mediated BMPR1B silencing was shown to play a key role in CSC maintenance in a subset of GBM (10), suggesting that BMPR1B might also be responsible for the decrease in tumorigenic potential in EZH2-silenced BT-CSC. However, we did not observe any effect of EZH2 depletion, either pharmacologic or shRNA mediated, on BMPR1B expression levels (Supplementary data 1*C*). Thus, the primary samples that we have tested probably do not belong to the subset of GBM in which BMPR1B is silenced by EZH2.

In summary, we have shown that pharmacologic and shRNA-mediated depletion of EZH2 in glioblastoma CSC reduces their ability to form new spheres *in vitro* and new tumors *in vivo*. We identified numerous transcripts that were regulated by the S-adenosylhomocysteine and EZH2 inhibitor DZNep and found *c-myc* to be one gene that is directly regulated by the PRC2 complex in CSC, explaining, at least in part, the mechanisms that

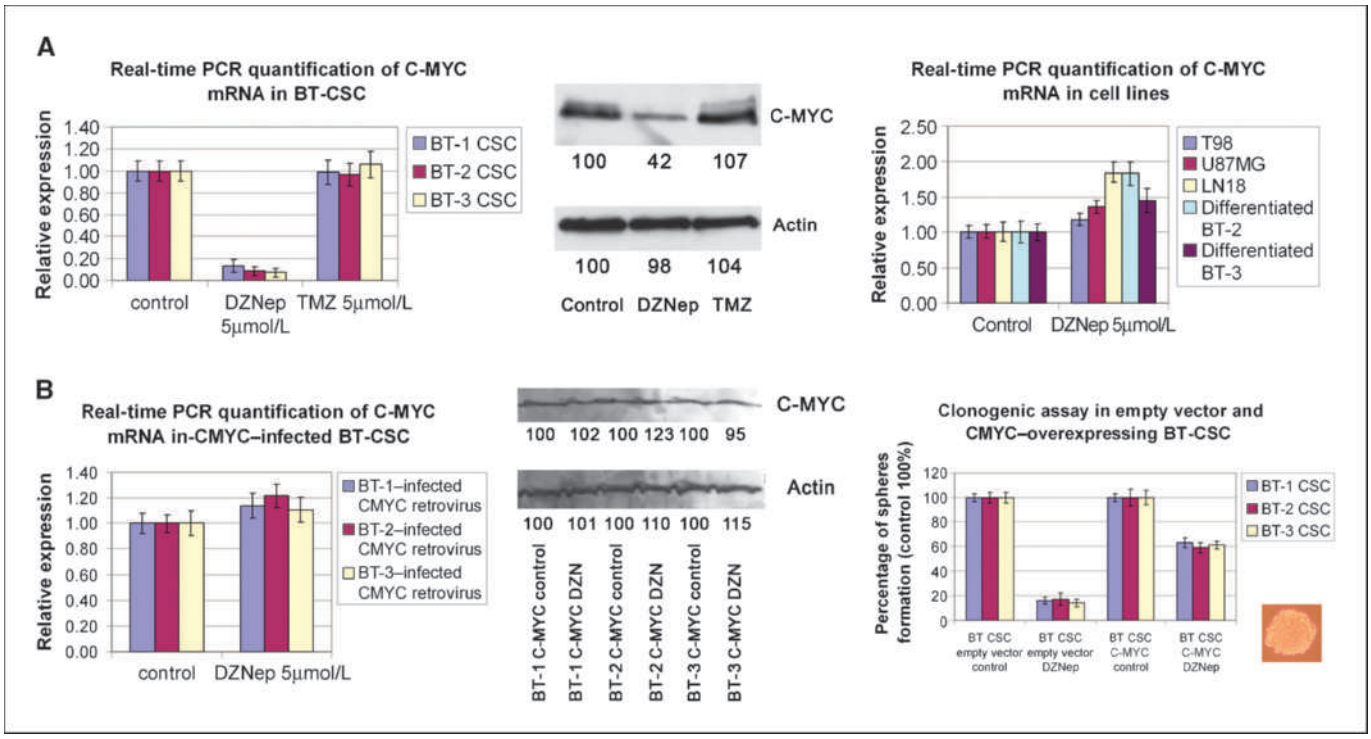

Figure 3. C-MYC is affected by pharmacologic disruption of EZH2 in GBM CSCs only and its exogenous expression partially rescues their clonogenic index. *A,* real-time PCR (*A, left*) and Western blot (*A, middle; numbers,* relative band intensity) analysis of c-myc expression showing a marked decrease of both transcript and protein in GBM CSC treated with 5 µmol/L DZNep, but not with temozolomide. Real-time PCR (*A, right*) analysis of c-myc expression in glioblastoma cell lines and partially differentiated CSCs showing no significant effect of DZNep on c-myc. *B,* real-time PCR (*B, left*) and Western blot (*B, middle*) analysis of c-myc expression in GBM CSC infected with a retrovirus expressing c-myc, showing no effect of DZNep on exogenous c-myc. *B, right,* clonogenic index in empty vector– and c-myc–overexpressing BT-CSC after DZNep treatment, showing a partial rescue of clonogenicity by exogenous c-myc expression. *Error bars,* SD of three independent determinations.

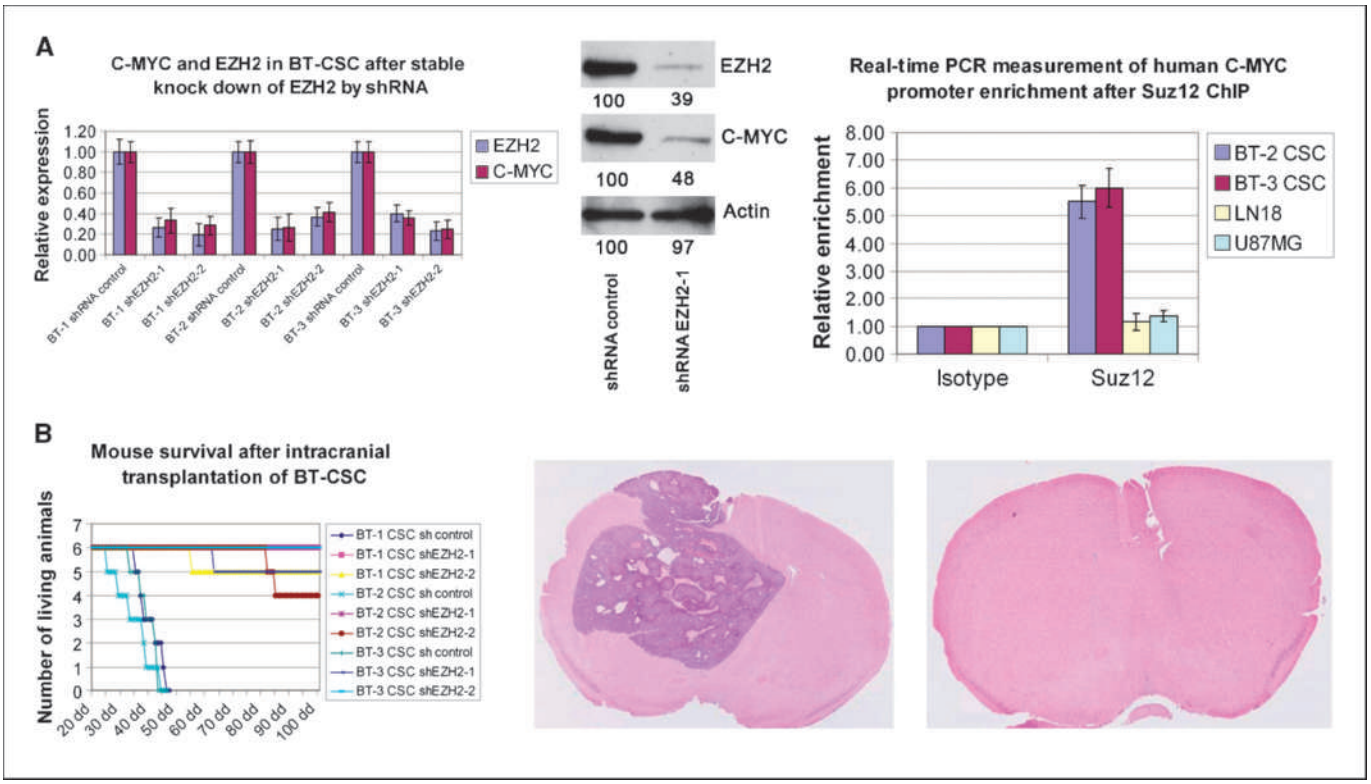

Figure 4. Downregulation of EZH2 by specific shRNA affects C-MYC expression level in GBM CSCs and strongly diminishes their tumor-forming capacity. *A,* specific shRNA-mediated downregulation of EZH2 in GBM CSC results in a strong reduction of c-myc transcript and protein levels, as assessed by real-time PCR (*A, left*) and Western blot analysis (*A, middle; numbers,* relative band intensity). *A, right,* ChIP experiments show the direct binding of SUZ12 to the c-myc promoter in GBM CSC but not in GBM cell lines. *Error bars,* SD of three independent determinations. *B, left,* survival of mice injected intracranially with three different GBM CSC populations, infected with viruses expressing either two EZH2-specific or control shRNA, showing that targeting EZH2 in GBM CSC results in a marked decrease of their tumor-initiating potential. Mice survival *P* values from log-rank test: EZH2-sh1 versus control: BT-1 (0.000506), BT-2 (0.000506), BT-3 (0.000759); EZH2-sh2 versus control: BT-1 (0.000506), BT-2 (0.000506), BT-3 (0.000759). *B, right,* histologic analysis, at day 35, of brains injected with control GBM CSC (*left*) or EZH2-depleted GBM CSC (*right*), illustrating the lack of tumor-forming ability upon EZH2 downregulation.

underlie the effect of EZH2 depletion on BT-CSC self-renewal and tumorigenicity. Our present work provides evidence that EZH2 depletion may constitute a prime therapeutic strategy for GBM, which, for now, remains an incurable malignancy.

Disclosure of Potential Conflicts of Interest

No potential conflicts of interest were disclosed.

Acknowledgments

Received 5/2/09; revised 9/22/09; accepted 10/16/09; published OnlineFirst 11/24/09.

Grant support: Fonds National de la Recherche Scientifique grant 3100A0-105833, OncoSuisse grant 01656-02-2005, and a grant from National Center of Competence in Research Molecular Oncology (I. Stamenkovic).

The costs of publication of this article were defrayed in part by the payment of page charges. This article must therefore be hereby marked *advertisement* in accordance with 18 U.S.C. Section 1734 solely to indicate this fact.

We thank Phil Shaw, Carlo Fusco, Marina Bacac, Claudio de Vito, Laetitia Mauti, and Anne Planche for insightful discussions.

References

1. Louis DN. Molecular pathology of malignant gliomas. Annu Rev Pathol 2006;1:97–117.
2. Stupp R, Mason WP, van den Bent MJ, et al. Radiotherapy plus concomitant and adjuvant temozolomide for glioblastoma. N Engl J Med 2005;352:987–96.
3. Galli R, Binda E, Orfanelli U, et al. Isolation and characterization of tumorigenic, stem-like neural precursors from human glioblastoma. Cancer Res 2004;64:7011–21.
4. Singh SK, Clarke ID, Terasaki M, et al. Identification of a cancer stem cell in human brain tumors. Cancer Res 2003;63:5821–8.
5. Singh SK, Hawkins C, Clarke ID, et al. Identification of human brain tumour initiating cells. Nature 2004;432:396–401.
6. Beier D, Hau P, Proescholdt M, et al. CD133(+) and CD133(−) glioblastoma-derived cancer stem cells show differential growth characteristics and molecular profiles. Cancer Res 2007;67:4010–5.
7. Dick JE. Stem cell concepts renew cancer research. Blood 2008;112:4793–807.
8. Bao S, Wu Q, McLendon RE, et al. Glioma stem cells promote radioresistance by preferential activation of the DNA damage response. Nature 2006;444:756–60.
9. Clement V, Sanchez P, de Tribolet N, Radovanovic I, Ruiz i Altaba A. HEDGEHOG-GLI1 signaling regulates human glioma growth, cancer stem cell self-renewal, and tumorigenicity. Curr Biol 2007;17:165–72.
10. Lee J, Son MJ, Woolard K, et al. Epigenetic-mediated dysfunction of the bone morphogenetic protein pathway inhibits differentiation of glioblastoma-initiating cells. Cancer Cell 2008;13:69–80.
11. Piccirillo SG, Reynolds BA, Zanetti N, et al. Bone morphogenetic proteins inhibit the tumorigenic potential of human brain tumour-initiating cells. Nature 2006;444:761–5.
12. Sparmann A, van Lohuizen M. Polycomb silencers control cell fate, development and cancer. Nat Rev Cancer 2006;6:846–56.
13. Bracken AP, Dietrich N, Pasini D, Hansen KH, Helin K. Genome-wide mapping of Polycomb target genes unravels their roles in cell fate transitions. Genes Dev 2006;20:1123–36.
14. Yu J, Rhodes DR, Tomlins SA, et al. A polycomb repression signature in metastatic prostate cancer predicts cancer outcome. Cancer Res 2007;67:10657–63.
15. Yu J, Cao Q, Mehra R, et al. Integrative genomics analysis reveals silencing of β-adrenergic signaling by polycomb in prostate cancer. Cancer Cell 2007;12:419–31.

16. Kotake Y, Cao R, Viatour P, Sage J, Zhang Y, Xiong Y. pRB family proteins are required for H3K27 trimethylation and Polycomb repression complexes binding to and silencing p16INK4α tumor suppressor gene. Genes Dev 2007;21:49–54.
17. O'Carroll D, Erhardt S, Pagani M, Barton SC, Surani MA, Jenuwein T. The polycomb-group gene Ezh2 is required for early mouse development. Mol Cell Biol 2001; 21:4330–6.
18. Boyer LA, Plath K, Zeitlinger J, et al. Polycomb complexes repress developmental regulators in murine embryonic stem cells. Nature 2006;441:349–53.
19. Tan J, Yang X, Zhuang L, et al. Pharmacologic disruption of Polycomb-repressive complex 2-mediated gene repression selectively induces apoptosis in cancer cells. Genes Dev 2007;21:1050–63.
20. Lee J, Kotliarova S, Kotliarov Y, et al. Tumor stem cells derived from glioblastomas cultured in bFGF and EGF more closely mirror the phenotype and genotype of primary tumors than do serum-cultured cell lines. Cancer Cell 2006;9:391–403.
21. Tseng CK, Marquez VE, Fuller RW, et al. Synthesis of 3-deazaneplanocin A, a powerful inhibitor of *S*-adenosylhomocysteine hydrolase with potent and selective *in vitro* and *in vivo* antiviral activities. J Med Chem 1989;32:1442–6.
22. Riggi N, Suva ML, Suva D, et al. EWS-FLI-1 expression triggers a Ewing's sarcoma initiation program in primary human mesenchymal stem cells. Cancer Res 2008;68:2176–85.
23. Bracken AP, Pasini D, Capra M, Prosperini E, Colli E, Helin K. EZH2 is downstream of the pRB-E2F pathway, essential for proliferation and amplified in cancer. EMBO J 2003;22:5323–35.
24. Beier D, Rohrl S, Pillai DR, et al. Temozolomide preferentially depletes cancer stem cells in glioblastoma. Cancer Res 2008;68:5706–15.
25. Wang J, Wang H, Li Z, et al. c-Myc is required for maintenance of glioma cancer stem cells. PLoS ONE 2008;3:e3769.
26. Zheng H, Ying H, Yan H, et al. p53 and Pten control neural and glioma stem/progenitor cell renewal and differentiation. Nature 2008;455:1129–33.
27. Wernig M, Meissner A, Foreman R, et al. *In vitro* reprogramming of fibroblasts into a pluripotent ES-cell-like state. Nature 2007;448:318–24.
28. Khan A, Shover W, Goodliffe JM. Su(z)2 antagonizes auto-repression of Myc in *Drosophila*, increasing Myc levels and subsequent trans-activation. PLoS ONE 2009;4:e5076.